



**HAL**  
open science

## Seasonal shift in airborne microbial communities

Romie Tignat-Perrier, Aurélien Dommergue, Alban Thollot, Olivier Magand,  
Pierre Amato, Muriel Joly, Karine Sellegri, Timothy M. Vogel, Catherine  
Larose

► **To cite this version:**

Romie Tignat-Perrier, Aurélien Dommergue, Alban Thollot, Olivier Magand, Pierre Amato, et al..  
Seasonal shift in airborne microbial communities. *Science of the Total Environment*, 2020, 716,  
pp.137129. 10.1016/j.scitotenv.2020.137129 . hal-02481717

**HAL Id: hal-02481717**

**<https://hal.science/hal-02481717v1>**

Submitted on 6 Nov 2020

**HAL** is a multi-disciplinary open access archive for the deposit and dissemination of scientific research documents, whether they are published or not. The documents may come from teaching and research institutions in France or abroad, or from public or private research centers.

L'archive ouverte pluridisciplinaire **HAL**, est destinée au dépôt et à la diffusion de documents scientifiques de niveau recherche, publiés ou non, émanant des établissements d'enseignement et de recherche français ou étrangers, des laboratoires publics ou privés.

# Seasonal shift in airborne microbial communities linked to land use

1  
2  
3  
4  
5  
6  
7  
8  
9  
10  
11  
12  
13  
14  
15  
16  
17  
18  
19  
20  
21  
22  
23  
24  
25

Romie Tignat-Perrier<sup>1,2\*</sup>, Aurélien Dommergue<sup>1</sup>, Alban Thollot<sup>1</sup>, Olivier Magand<sup>1</sup>, Pierre Amato<sup>3</sup>, Muriel Joly<sup>3</sup>, Karine Sellegri<sup>3</sup>, Timothy M. Vogel<sup>2</sup>, Catherine Larose<sup>2</sup>

<sup>1</sup>Institut des Géosciences de l'Environnement, Université Grenoble Alpes, CNRS, IRD, Grenoble INP, Grenoble, France

<sup>2</sup>Environmental Microbial Genomics, CNRS UMR 5005 Laboratoire Ampère, École Centrale de Lyon, Université de Lyon, Écully, France

<sup>3</sup>Institut de Chimie de Clermont-Ferrand, CNRS UMR 6096 Université Clermont Auvergne-Sigma, Clermont-Ferrand, France

[\\*romie.tignat@univ-grenoble-alpes.fr](mailto:*romie.tignat@univ-grenoble-alpes.fr)

## Highlights

-Airborne microbial communities showed a seasonal shift at the puy de Dôme elevated site

-Dominant microbial taxa showed different trends throughout the year

-Summer results in higher concentrations of plant-associated microbes in the air

-Winter results in higher concentrations of soil and dead material-associated microbes

-Seasonal changes in the underlying ecosystems likely drive microbial seasonal shift

## Abstract

26 Microorganisms are ubiquitous in the atmosphere. Global investigations on the geographical  
27 and temporal distribution of airborne microbial communities are critical for identifying the  
28 sources and the factors shaping airborne communities. At mid-latitude sites, a seasonal shift in  
29 both the concentration and diversity of airborne microbial communities has been  
30 systematically observed in the planetary boundary layer. While the factors suspected of  
31 affecting this seasonal change were hypothesized (*e.g.*, changes in the surface conditions,  
32 meteorological parameters and global air circulation), our understanding on how these factors  
33 influence the temporal variation of airborne microbial communities, especially at the  
34 microbial taxon level, remains limited. Here, we investigated the distribution of both airborne  
35 bacterial and fungal communities on a weekly basis over more than one year at the mid-  
36 latitude and continental site of puy de Dôme (France; +1465 m altitude above sea level). **The**  
37 **seasonal shift in microbial community structure was likely correlated to the seasonal changes**  
38 **in the characteristics of puy de Dôme's landscape** (croplands and natural vegetation). The  
39 airborne microbial taxa that were the most affected by seasonal changes trended differently  
40 throughout the seasons in relation with their trophic mode. In addition, the windy and variable  
41 local meteorological conditions found at puy de Dôme were likely responsible for the  
42 intraseasonal variability observed in the composition of airborne microbial communities.

43

44 Keywords: atmospheric microorganisms, bioaerosols, planetary boundary layer, amplicon  
45 sequencing, biosphere-atmosphere interactions

46

## 47 Introduction

48 Thousands to millions of diverse microbial cells per cubic meter of air are transported among  
49 aerosols with their diversity shown to depend on geographic location<sup>1</sup> and time of year<sup>2</sup>.  
50 These microorganisms might be active, since some airborne microbial isolates were shown in

51 laboratory studies to sustain metabolic activity using organic acids found in the atmosphere<sup>3-5</sup>.  
52 Understanding the global distribution of airborne microbial communities is critical for  
53 determining how airborne microorganisms might influence atmospheric chemistry<sup>4</sup>,  
54 meteorological processes such as cloud and precipitation formation<sup>6</sup>, as well as human and  
55 crop health<sup>7</sup>. Recent large geographical and spatial investigations highlighted the major  
56 contribution of the local landscapes and local environmental factors in the observed  
57 distribution of airborne microbial communities in the planetary boundary layer<sup>1,8</sup>. The  
58 composition of airborne microbial communities is closely related to the nature of the  
59 surrounding landscapes (ocean, agricultural soil, forest *etc.*) from which local meteorology  
60 (especially wind direction and speed) controls microbial cell emission rates<sup>1</sup>. Studies on  
61 airborne microbial communities at mid-latitude sites (aerosol-, cloud water- and precipitation-  
62 associated microorganisms) reported seasonal changes in both microbial biomass and  
63 biodiversity<sup>2,9-13</sup>. The seasonal variability was associated to changes in surface conditions<sup>10,11</sup>,  
64 meteorological conditions<sup>2,9</sup> and/or changes in the global air circulation<sup>9,13</sup>. Yet, our  
65 understanding on how these potential factors impact airborne microbial community  
66 composition, and more specifically the microbial taxa individually, remains limited. Here, we  
67 investigated the distribution of airborne microbial communities and specific microbial taxa at  
68 the mid-latitude and continental site of puy de Dôme (France; +1465 m altitude above sea  
69 level). We monitored the diversity and abundance of bacterial and fungal communities in the  
70 troposphere on a weekly basis for more than a year (June 2016 to August 2017). **These**  
71 **microbial community metrics were evaluated in relation to the local meteorology and**  
72 **particulate matter chemical composition, and puy de Dôme local landscape was evaluated**  
73 **based on the MODIS satellite images.** While a number of studies focusing on microorganisms  
74 in clouds has been carried out at puy de Dôme<sup>3,4,14-17</sup>, no investigation was conducted in the  
75 dry troposphere and at such a high temporal resolution. Puy de Dôme is surrounded mainly by

76 croplands and vegetation (*i.e.* > 80% of the surrounding landscapes in a perimeter of 50 km)  
77 whose surface characteristics change drastically over the four different seasons (summer,  
78 autumn, winter and spring). These seasonal changes in landscape were related to the temporal  
79 variability of airborne microbial community composition at the microbial taxon level.

80

## 81 Material and Methods

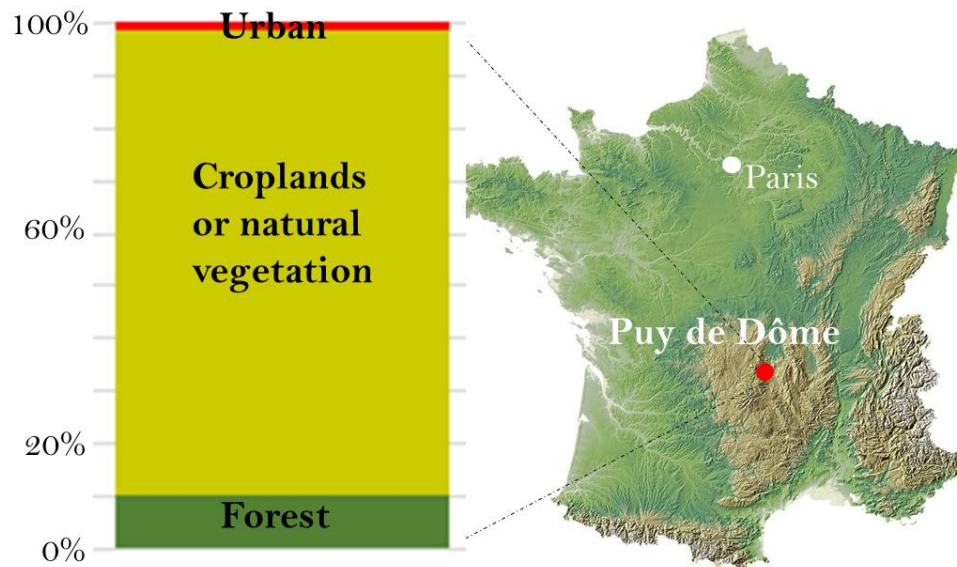
### 82 *Sites and Sampling*

83 A size selective high volume air sampler installed at the puy de Dôme (PDD) meteorological  
84 station terrace was used to collect particulate matter on quartz fiber filters every week from  
85 June 2016 to August 2017 (**Table S1**). The sampler was equipped with a PM10 size-selective  
86 inlet in order to collect particulate matter smaller than 10 µm (PM10) and sampling was done  
87 as presented in Dommergue et al. (2019)<sup>18</sup>. Overall, the dataset was composed of fifty-three  
88 samples with an average normalized collected volume of 9100 m<sup>3</sup> (**Table S1**). Quartz fiber  
89 filters were heated to 500°C for 8 hours to remove traces of organic carbon including DNA.  
90 All the material including the filter holders, aluminium foils and plastic bags in which the  
91 filters were transported were sterilized using UV radiation as detailed in Dommergue et al.,  
92 (2019)<sup>18</sup>. A series of field and transportation blank filters were carried out to monitor the  
93 quality of the sampling protocol as presented in Dommergue et al. (2019)<sup>18</sup>. PDD is a mid-  
94 altitude (+ 1465 m) site surrounded by croplands, an urban area (Clermont-Ferrand) and  
95 forests within a 50 km perimeter (**Fig. 1**). Monthly NASA satellite images of puy de Dôme  
96 surrounding surfaces (<https://wvs.earthdata.nasa.gov/>) are shown in **Fig. S1**. The Atlantic  
97 coast and Mediterranean Sea are at around 320 km and 240 km from PDD, respectively.

98

99

100



101

102 **Fig. 1. Geographical location and landscape of the sampling site.** Map showing the  
 103 location of the puy de Dôme mountain in France and relative surfaces types surrounding the  
 104 site in a perimeter of 50 km based on the MODIS satellite images. Cropland and vegetation  
 105 areas comprise > 80% of the surrounding landscapes, while forest and urban areas (mainly  
 106 Clermont-Ferrand) comprise < 20% of the surrounding landscapes.

107

108

109 *DNA extraction*

110 We extracted DNA from 3 punches (diameter of one punch: 38 mm) from the quartz fiber  
 111 filters using the DNeasy PowerWater kit with some modifications as detailed in Dommergue  
 112 et al. (2019)<sup>18</sup>. During cell lysis, an one hour heating step at 65°C followed by a 10-min  
 113 vortex treatment at maximum speed and a centrifugation using a syringe to separate the filter  
 114 debris from the lysate were added to the DNeasy PowerWater DNA extraction protocol<sup>18</sup>.  
 115 DNA concentration was measured using the High Sensitive Qubit Fluorometric  
 116 Quantification (Thermo Fisher Scientific) then stored at -20°C.

117

118 *Real-Time qPCR analyses*

119 The bacterial cell concentration was approximated by the number of 16S rRNA gene copies  
120 per cubic meter of air and the fungal cell concentration was approximated by the number of  
121 18S rRNA gene copies per cubic meter of air. Primers and methodology are presented in  
122 Tignat-Perrier et al. (2019)<sup>1</sup>.

123

124 *MiSeq Illumina amplicon sequencing*

125 ***16S rRNA gene sequencing: library preparation, reads quality filtering and taxonomic***  
126 ***annotation.*** The V3-V4 region of the 16S rRNA gene was amplified and libraries were  
127 prepared as presented in Tignat-Perrier et al. (2019)<sup>1</sup>. The amplicons were sequenced by  
128 paired-end MiSeq sequencing using the V3 Illumina technology with 2 x 250 cycles. Reads  
129 were filtered based on quality using FASTX-Toolkit  
130 ([http://hannonlab.cshl.edu/fastx\\_toolkit/](http://hannonlab.cshl.edu/fastx_toolkit/)), assembled using PANDAseq<sup>19</sup>, and annotated using  
131 RDP Classifier<sup>20</sup> and the RDP 16srRNA database as detailed in Tignat-Perrier et al. (2019)<sup>1</sup>.  
132 RDP classifier was used in part to avoid errors due to sequence clustering. The number of  
133 sequences per sample and the percentage of sequences annotated at the genus level were  
134 evaluated using a home-made R script. The sequences annotated as chloroplasts by RDP were  
135 manually removed.

136 ***ITS rRNA gene sequencing: library preparation, reads quality filtering and taxonomic***  
137 ***annotation.*** The ITS2 region of the ITS was amplified libraries were prepared as presented in  
138 Tignat-Perrier et al. (2019)<sup>1</sup>. The amplicons were sequenced by a paired-end MiSeq  
139 sequencing using the technology V2 of Illumina with 2 x 250 cycles. Reads were filtered  
140 based on quality using FASTX-Toolkit, assembled using PANDAseq, and annotated at the  
141 species level<sup>21</sup> using RDP Classifier and the RDP fungallsu database as detailed in Tignat-  
142 Perrier et al. (2019)<sup>1</sup>. The number of sequences per sample and the percentage of sequences  
143 annotated at the species level were evaluated using a home-made R script.

144 The number of reads per sample and per sequencing (V3-V4 regions of the 16S rRNA gene  
145 and the ITS2 region of the ITS) is presented in the **Table S1**. Samples with less than 6000  
146 reads were removed. Samples from the same season were pooled and rarefaction curves per  
147 season were done (**Fig. S2**).

148

#### 149 *Estimation of the trophic mode of the fungal species*

150 We used the FUNGuild software<sup>22</sup> to assign the trophic mode of the fungal species (RDP  
151 classifier based annotation). Fungal species annotated to a trophic mode with the level  
152 confidence “Possible” were grouped in the “not classified” fungi. Then, we calculated the  
153 percentage represented by each trophic mode per sample. Heatmaps were done using the R  
154 package gplots.

155

#### 156 *Chemical analyses*

157 The elemental carbon (EC), organic carbon (OC), sugar anhydrides and alcohols  
158 (levoglucosan, mannosan, galactosan, inositol, glycerol, erythriol, xylitol, arabitol, sorbitol,  
159 mannitol, trehalose, rhamnose, glucose, fructose and sucrose), soluble anions (MSA,  $\text{SO}_4^{2-}$ ,  
160  $\text{NO}_3^-$ ,  $\text{Cl}^-$ , Ox) and cations ( $\text{Na}^+$ ,  $\text{NH}_4^+$ ,  $\text{K}^+$ ,  $\text{Mg}^{2+}$ ,  $\text{Ca}^{2+}$ ) concentrations were analyzed as  
161 presented in Dommergue et al. (2019)<sup>18</sup>.

162

#### 163 *Meteorological data*

164 Meteorological parameters such as wind speed and direction, temperature, relative humidity  
165 and UV were collected (Vaisala instrument). For each sample, the backtrajectories of the air  
166 masses were calculated over 3 days before the sampling using HYSPLIT<sup>23</sup> (maximum height  
167 above ground level: 1 km).

168



169 *Graphical and Statistical analyses*

170 *Environmental variables.* For chemical species, air concentrations in ng per cubic meter of air  
171 were used in the analyses. The chemical table was log10-transformed to approach a Gaussian  
172 distribution (verified on a Q-Q plot and tested using the Shapiro-Wilk test), and a hierarchical  
173 cluster analysis (average method) was done on the Euclidean distance matrix using the vegan  
174 and ade4 R packages. Meteorological data were used to do the wind roses using the openair R  
175 package<sup>24</sup>. Backtrajectories of the air masses over three days were plotted on maps using the  
176 openair R package, and the relative surfaces of the landscapes (MODIS land surfaces) air  
177 masses over flown were calculated.

178 *Diversity statistics and Multivariate analyses.* Before doing the multivariate analyses, the raw  
179 abundances of the taxa (bacterial genera and fungal species) were transformed into relative  
180 abundances to counter the heterogeneity in the number of sequences per sample. A  
181 hierarchical cluster analysis (average metric) on the Bray-Curtis dissimilarity matrix was done  
182 using the vegan and ade4 R packages<sup>25</sup>. We have defined the seasons as following: we  
183 adjusted the beginning and ending administrative dates of the seasons (*i.e.* summer: 20<sup>th</sup> of  
184 June to 22<sup>th</sup> of September; autumn: 23<sup>th</sup> of September to 21<sup>th</sup> of December; winter: 22<sup>th</sup> of  
185 December to 19<sup>th</sup> of March; spring: 20<sup>th</sup> of March to 19<sup>th</sup> of June) based on the weekly mean  
186 temperature (**Fig. S3**). France goes through a cycle of four strong seasons characterized by  
187 distinctive weather: the summer is characterized by higher temperatures, a longer daylight  
188 period and the period of fructification of fruiting plants; the autumn is the harvest period of  
189 most annual crops and a preparation period for dormancy; winter is characterized by the  
190 lowest temperatures, frequent precipitation (rain and snow) and high air humidity; and finally  
191 the spring is characterized by milder weather, snow melting, budding and flowering. To  
192 access the variability of microbial population structure within the seasons, we averaged the  
193 degrees of dissimilarity obtained from the Bray-Curtis matrix for each pair of samples from

194 the same season, subtracted these values from 1 to get similarity values and divided the  
195 similarity values by the standard deviation (as detailed in Tignat-Perrier et al., 2019<sup>1</sup>).  
196 Spearman correlations were calculated to test the correlation between microbial abundance  
197 and richness and quantitative environmental factors using the Hmisc R package<sup>26</sup>. ANOVA  
198 analyses were used to test the influence of qualitative factors such as season and year on both  
199 bacterial and fungal abundance and richness using the vegan R package, followed by  
200 TukeyHSD tests to identify which group revealed a significantly different mean. A distance-  
201 based redundancy analysis (RDA – linear or non-linear correlation) was carried out to  
202 evaluate the part of the variance between the samples explained by the seasons, chemistry  
203 and/or meteorology, and an ANOVA was carried out to test each variable using the vegan and  
204 ade4 R packages. Venn diagrams using the R package VennDiagram were done to access the  
205 shared and unique bacterial genera and fungal species from each season after rarefaction on  
206 the raw abundances (rarefaction at the minimum number of reads). A Mantel test between the  
207 Bray-Curtis matrices based on the bacterial genera and fungal species was used to evaluate  
208 similarities in the distribution of the samples. A Mantel test was done between the Bray-Curtis  
209 matrix based on either the bacterial or the fungal diversity and the Euclidean distance matrix  
210 based on the chemical variables or meteorology to evaluate the similarities in the distribution  
211 of the samples.

212

213

## 214 Results

### 215 *Temporal distribution of airborne microbial communities*

216 *Airborne microbial abundance.* Airborne bacterial and fungal concentrations (estimated by  
217 the number of 16S rRNA and 18S rRNA gene copies) were positively correlated ( $r=0.77$ ,  
218  $p\text{value}=7.9 \times 10^{-11}$ ) and varied between  $1.8 \times 10^3$  and  $2.1 \times 10^7$  cells per cubic meter of air and 3

219 and  $1.0 \times 10^5$  cells per cubic meter of air, respectively. Neither bacteria nor fungal abundance  
 220 significantly varied with season (pvalues=0.20 and 0.38, respectively), but the highest  
 221 concentrations observed occurred in spring and summer for both bacteria and fungi (**Table 1**  
 222 and **Fig. S4**).

223

224 **Table 1. Microbial concentration and richness estimations depending on the season.**

225 Concentrations of bacterial and fungal ribosomal gene copies and associated richness (number  
 226 of bacterial genera and fungal species) averaged for each season and relative standard  
 227 deviation. Reference letters indicate the group membership based on Tukey's HSD post hoc  
 228 tests (done only for the estimated bacterial richness as the ANOVA showed differences  
 229 between the groups).

Season	Average bacterial concentration (number of 16S rRNA gene copies/m <sup>3</sup> of air)	Average fungal concentration (number of 18S rRNA gene copies/m <sup>3</sup> of air)	Average Chao1 bacterial richness estimation (estimated number of bacterial genera)	Average Chao1 fungal richness estimation (estimated number of fungal species)
PDD spring	$2.7 \times 10^6 \pm 6.2 \times 10^6$	$4.6 \times 10^3 \pm 1.1 \times 10^4$	$4.8 \times 10^2 \pm 1.4 \times 10^{2\ ab}$	$4.7 \times 10^2 \pm 9.3 \times 10^1$
PDD summer	$8.5 \times 10^5 \pm 1.3 \times 10^6$	$1.6 \times 10^4 \pm 2.8 \times 10^4$	$6.1 \times 10^2 \pm 1.5 \times 10^{2\ a}$	$4.6 \times 10^2 \pm 1.9 \times 10^2$
PDD autumn	$2.2 \times 10^5 \pm 4.0 \times 10^5$	$3.2 \times 10^3 \pm 4.6 \times 10^3$	$4.3 \times 10^2 \pm 1.2 \times 10^{2\ b}$	$3.6 \times 10^2 \pm 1.9 \times 10^2$
PDD winter	$3.6 \times 10^5 \pm 9.0 \times 10^5$	$7.4 \times 10^2 \pm 9.4 \times 10^2$	$3.9 \times 10^2 \pm 1.4 \times 10^{2\ b}$	$3.0 \times 10^2 \pm 1.8 \times 10^2$

230

231 *Airborne microbial richness.* The observed richness varied between 150 and 674 genera of  
 232 bacteria, and 84 and 649 species of fungi. The estimated richness (Chao1) varied between 234  
 233 and 897 bacterial genera and 97 and 820 fungal species. The estimated bacterial richness was  
 234 higher in summer compared to winter and autumn (pvalue= $4.5 \times 10^{-4}$ ; **Table 1**). The estimated  
 235 fungal richness also was highest in summer, while not significant due to relatively higher

236 variability (pvalue=0.18; **Table 1**). A rough correlation was found between the estimated  
237 richness estimations and concentration estimations for both bacteria and fungi (r=0.41,  
238 pvalue= $3.0 \times 10^{-3}$  and r=0.50, pvalue= $4.6 \times 10^{-4}$ , respectively).

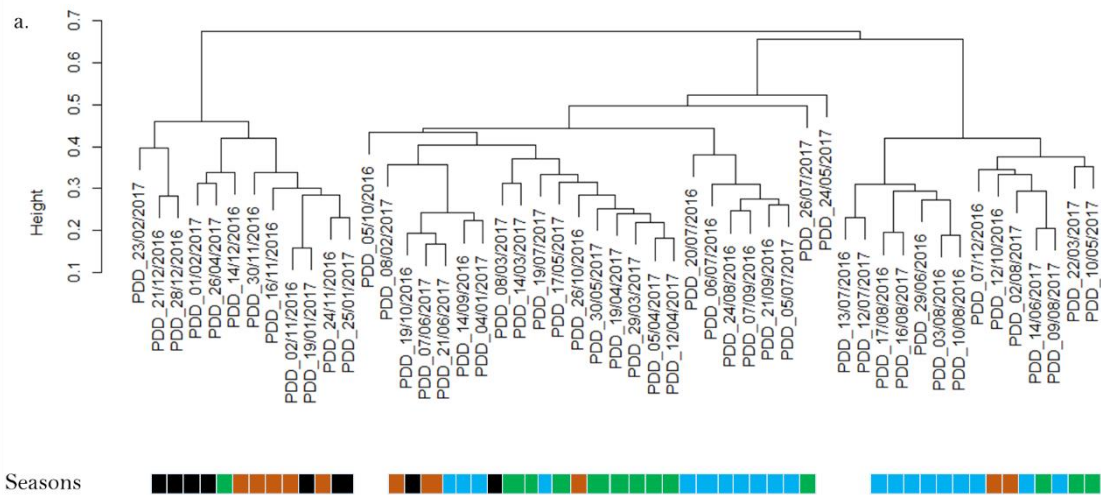
239 Consistently with highest richness, summer had the highest percentage of unique bacterial  
240 genera (16% or 198/1239 of the genera in summer were only present in this season), followed  
241 by autumn (4.5% or 39/873), spring (4.4% or 42/953) and winter (4.3% or 37/864) (**Fig. S5**).  
242 This was also observed for unique fungal species with the highest percentage observed in  
243 summer (28.4% or 457/1606), followed by autumn (17.4% or 191/1097), spring (14.4% or  
244 172/1196) and winter (8% or 63/786) (**Fig. S5**). The majority of the bacterial genera and  
245 fungal species observed was present throughout the year, (*i.e.* they were shared by all the  
246 seasons; **Fig. S5**).

247 The five most abundant bacterial genera were *Bacillus* (15.6% in average) (Firmicutes),  
248 *Hymenobacter* (9.2%) (Bacteroidetes), *Sphingomonas* (7.4%) (Alphaproteobacteria),  
249 *Methylobacterium* (5.1%) (Alphaproteobacteria) and *Thermoactinomyces* (4.6%)  
250 (Firmicutes). Their relative abundance varied over the year: *Bacillus* was abundant throughout  
251 the year and dominated the community from summer to spring, while *Hymenobacter*  
252 increased in autumn and winter (19.2% and 13.9% respectively). The twenty-five most  
253 abundant bacterial genera and fungal species observed in each season are listed in **Table S2**.  
254 In fungi, the five most abundant species were *Pseudotaeniolina globosa* (11.5% in average),  
255 *Cladophialophora proteae* (7.9%), *Alternaria* sp. BMP\_2012 (4%), *Cladophialophora*  
256 *minutissima* (4%) and *Naevula minutissima* (3.1%). Similar to bacteria, their relative  
257 abundance varied seasonally: *Cladophialophora proteae* represented 13.3% of the community  
258 in winter and only 0.3% in summer, when *Alternaria* dominated (10.8%); autumn was  
259 dominated by *Pseudotaeniolina globosa* and *Cladophialophora proteae* (16.4% and 15.6%,

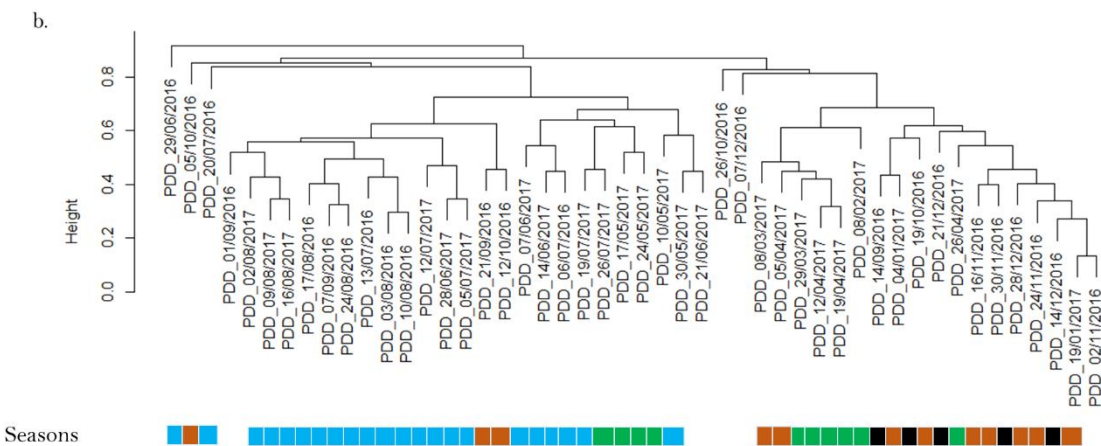
260 respectively), while *Naevala minutissima* was detected only in spring and summer,  
261 dominating in spring (10.1%).

262 *Airborne microbial structure.* The hierarchical cluster analyses of the samples based on both  
263 the bacterial (genus level) and fungal (species level) community structures are shown in **Fig.**  
264 **2**; these were highly similar ( $r=0.50$  and  $pvalue<0.001$ ). The samples tended to group by  
265 season (anosim  $r=0.30$  and  $r=0.49$  with  $pvalues=0.001$  for bacterial and for fungal  
266 communities, respectively; **Fig. 2**) with season explaining 17% and 22% of the variability in  
267 the community structures, respectively ( $pvalues=0.001$ ). The distribution of the summer  
268 samples based on fungal species was different between 2016 and 2017 ( $pvalue=0.001$ ). The  
269 intraseasonal variability in community structure was greatest in spring and smallest in  
270 summer for bacteria and conversely greatest in autumn and smallest in winter for fungi  
271 (**Table S3**). The relative abundances of fungal saprotrophs and symbiotrophs (like *Balospora*  
272 *myosura*, *Strobilurus albipilatus*, *Pseudotaeniolina globosa*) (**Fig. 3**) were greater in autumn  
273 and winter than during the rest of the year ( $pvalue=4.3 \times 10^{-5}$  and 0.5 for saprotrophs and  
274 symbiotrophs, respectively). The relative abundance of fungal pathotrophs was greater in the  
275 spring and summer periods ( $pvalue=0.51$  – **Fig. 3**). Examples of phytopathogens increasing in  
276 relative abundance during the summer and/or spring are *Mycosphaerella graminicola* (wheat  
277 plant pathogen – **Fig. S6**), *Microdochium majus* (cereal pathogen – **Fig. S6**), *Blumeria*  
278 *graminis* (powdery mildew pathogen – **Fig. S6**), *Ustilago hordei* (maize pathogen – **Fig. S6**),  
279 *Botryotinia fuckeliana* (gray mold disease) and *Erysiphe alphitoides* (powdery mildew on oak  
280 trees). However, the number of fungal species associated to pathogenic and saprophytic  
281 trophic modes was greatest in spring and summer, whereas symbiotrophs were mostly found  
282 in summer and autumn (**Table S4**).

283



284



285

286 ■ Spring ■ Summer ■ Autumn ■ Winter

287

**Fig. 2. Distribution of the samples based on the microbial community structure.**

288 Hierarchical cluster analysis (average method) of airborne community structures of bacteria

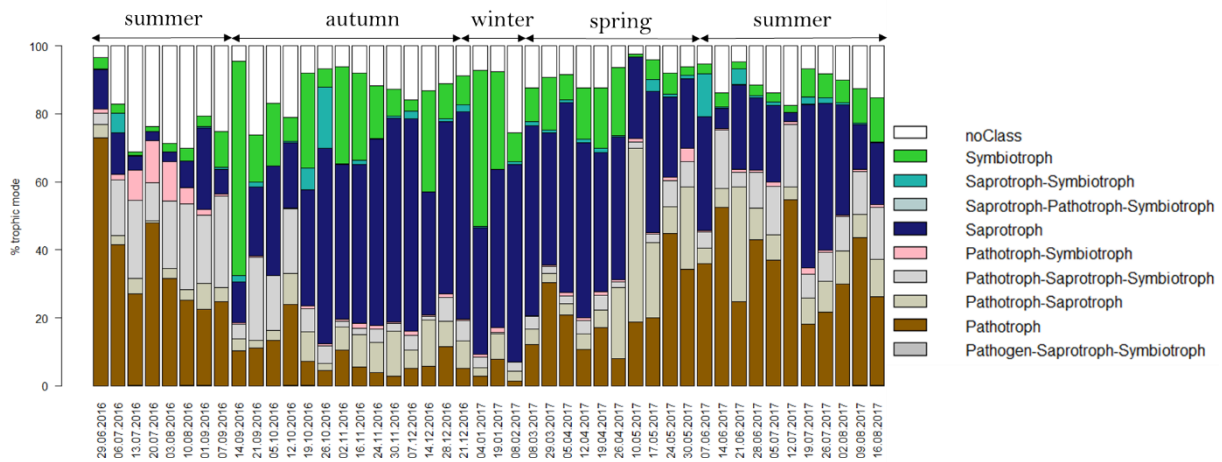
289 (16S rRNA gene – a.) and fungi (ITS region – b.) based on Bray-Curtis dissimilarity matrices.

290 The season corresponding to each sample is indicated as a frieze (black=winter,

291 blue=summer, green=spring and brown=autumn) that has been split into three based on the

292 three major clusters observed on the hierarchical cluster analyses.

293



294

295 **Fig. 3. Distribution of the trophic modes of the fungal species identified.** Each fungal  
 296 species detected was associated to either a specific trophic mode, different trophic modes or  
 297 no trophic mode (« noClass ») using the FUNGuild software, then the proportions of species  
 298 belonging to each trophic mode were summed.

299

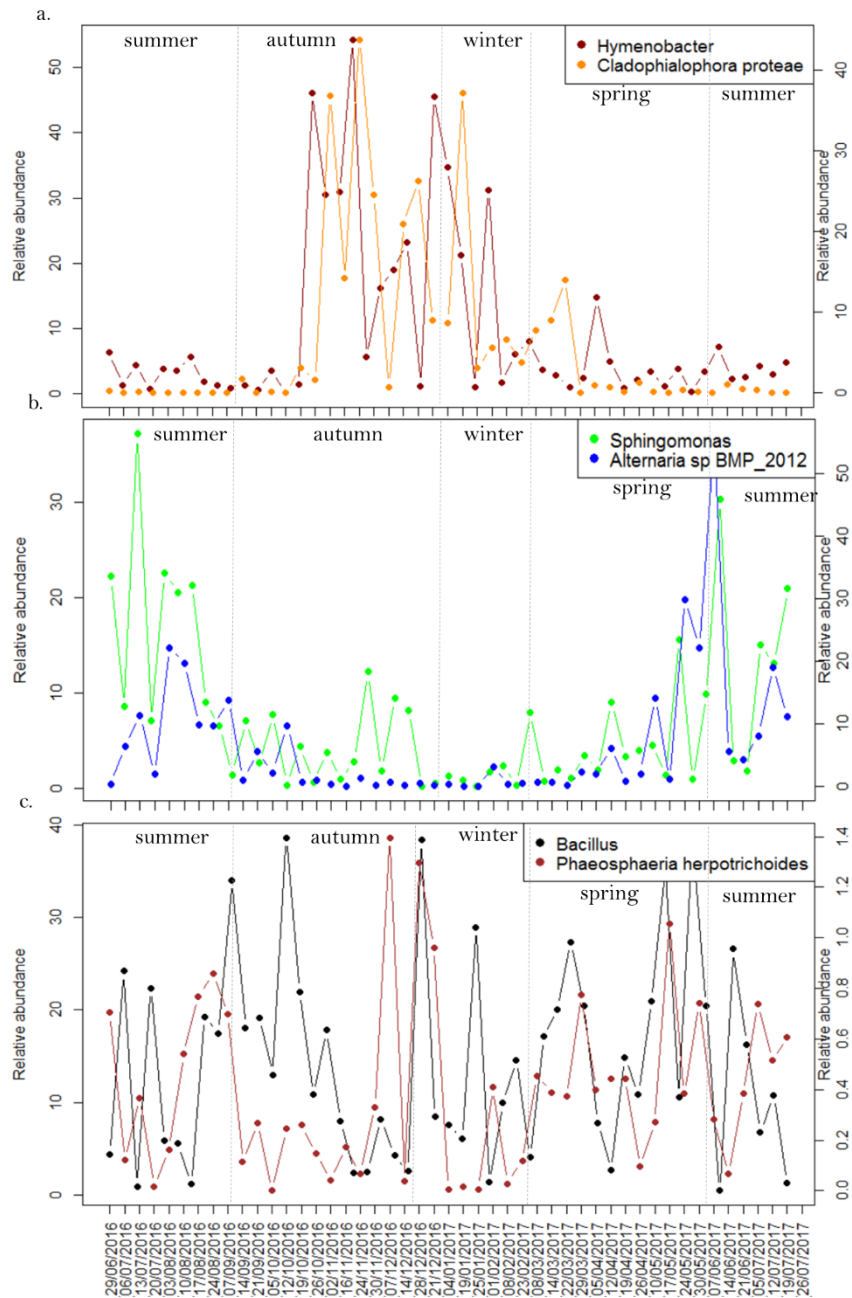
300

301 When looking at the fifty most abundant bacterial genera and fungal species of the dataset that  
 302 mainly controlled the distribution of the samples based on the microbial community structure  
 303 (they represented 79.6% or 881898 sequences/1107323 and 71.8% or 367440  
 304 sequences/511738 of all the bacterial and fungal sequences, respectively), we observed three  
 305 different patterns in the temporal variation of their relative abundance (**Fig. 4** and **5**). The  
 306 period during which the relative abundance increased varied in length and depended on the  
 307 microorganism. First, some taxa were mostly abundant during the cold period of the year:  
 308 20% (10/50) of the bacterial genera and 34% (17/50) of the fungal species showed a higher  
 309 relative abundance in winter and/or autumn compared to the other seasons. This was the case  
 310 with *Hymenobacter* and *Pseudotaeniolina proteae* for example, whose relative abundances  
 311 suddenly increased between November 2016 and February 2017, and between October 2016  
 312 and April 2017, respectively (**Fig. 4a**). Fungal taxa belonging to this group were almost

313 exclusively saprotroph and/or pathotroph (**Table S5**). Second, some taxa were mostly  
314 abundant during summer and/or spring: 42% (21/50) of the bacterial genera and 46% (23/50)  
315 of the fungal species. For example, *Sphingomonas* and *Alternaria* sp. BMP\_2012 relative  
316 abundances started to decrease in late summer/early autumn and increased again in the late  
317 spring (**Fig. 4b**). Fungal taxa belonging to this group were pathotroph, symbiotroph or  
318 saprotroph (**Table S5**). Finally, some taxa had no clear pattern in their relative abundance (*i.e.*  
319 stable or randomly variable over the year): 38% (19/50) of the bacterial genera and 20%  
320 (10/50) of the fungal species (e.g., *Bacillus* and *Phaeosphaeria herpotrichoides*) (**Fig. 4c**).  
321 Fungal taxa belonging to this group were mostly saprotroph (**Table S5**).

322





323

324

325 **Fig. 4. Temporal evolution of the relative abundance of several fungal species and**  
 326 **bacterial genera among the airborne communities over the year.**

327 a) Higher relative abundance in autumn and winter: examples of the fungal species  
 328 *Cladophialophora proteae* (right y scale) and the bacterial genus *Hymenobacter* (left y  
 329 scale);

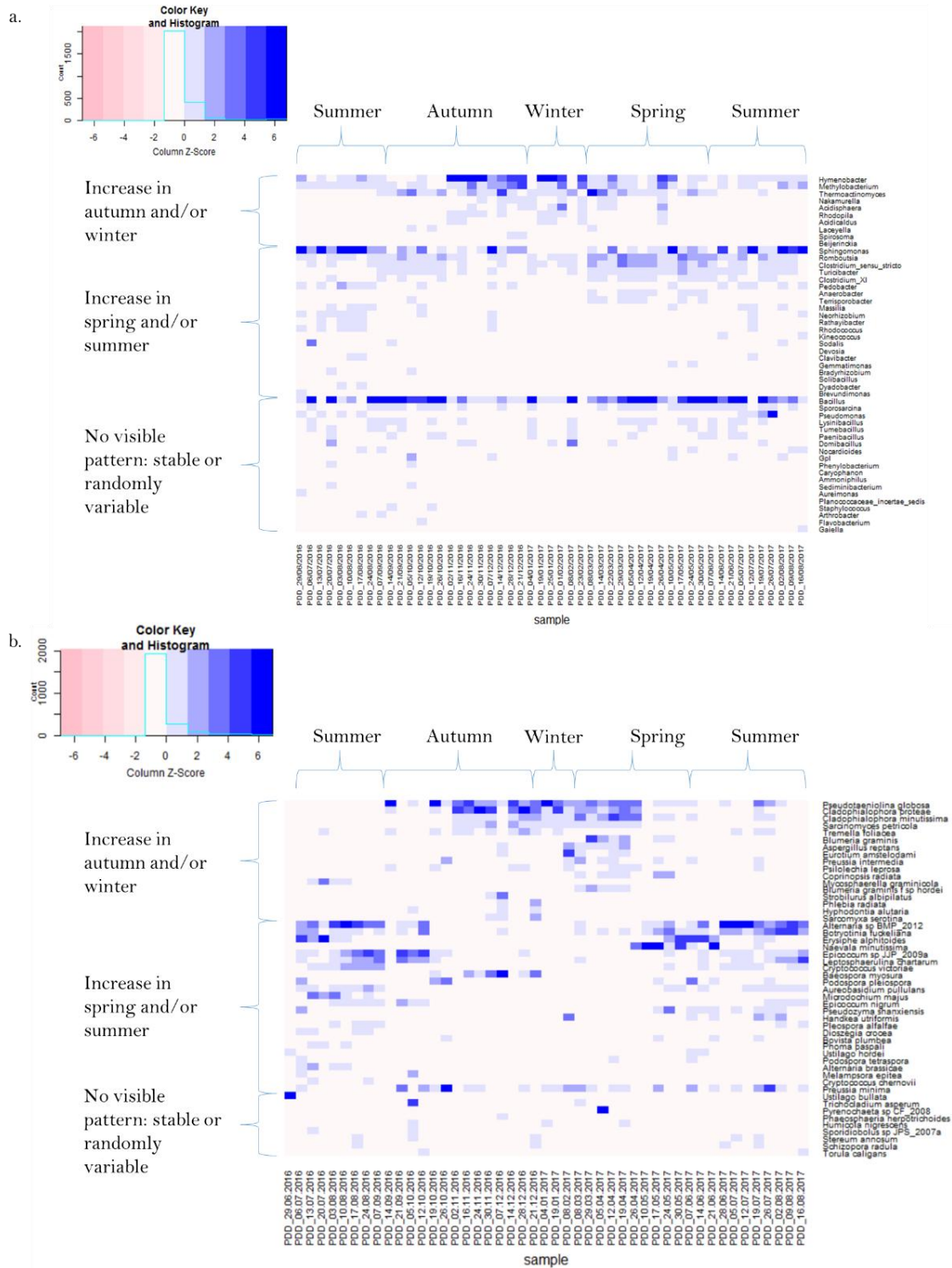
330 b) Higher relative abundance in spring and summer: examples of the fungal species  
331 *Alternaria* sp. BMP 2012 (right y scale) and the bacterial genus *Sphingomonas* (left y  
332 scale);

333 c) No trend of the relative abundance over the year: examples of the fungal species  
334 *Phaeosphaeria herpotrichoides* (right y scale) and the bacterial genus *Bacillus* (left y  
335 scale).

336

337

338



339

340 **Fig. 5. Temporal evolution of the relative abundances of the dominant microbial taxa.**

341 Heatmaps showing the temporal evolution of the relative abundances (centered and scaled) of

342 the fifty most abundant bacterial genera (a.) and fungal species (b.) in the dataset. The

343 microbial taxa are grouped based on the three general trends exemplified in **Fig. 4.**

344

345

### 346 *Atmospheric PM10 chemistry*

347 The hierarchical cluster analysis of the samples based on the PM10 chemical profile is shown  
348 in **Fig. S7**. Chemical concentrations varied significantly with season (pvalues<0.05) for all the  
349 compounds measured except  $\text{Cl}^-$ ,  $\text{NO}_3^-$ ,  $\text{NH}_4^+$  and rhamnose (pvalues>0.05) (**Table S6**).  
350 Seasons explained 38% of the variance in the distribution of the samples based on the  
351 chemical composition (pvalue=0.001). When looking at the weekly variation of the  
352 concentrations of the different compounds, we observed general trends of seasonal variations  
353 (as observed for microbial communities). Some increased during autumn/winter compared to  
354 spring/summer (galactosan, levoglucosan and mannosan), while some others decreased  
355 (erythriol, glucose, trehalose, sorbitol, xylitol, inositol,  $\text{SO}_4^{2-}$ , OC, MSA) (**Fig. S8**). The  
356 sample distribution based on bacterial and fungal community structures were correlated to  
357 their distribution based on the overall PM10 chemistry (Mantel test  $r=0.25$  pvalue=0.001 and  
358  $0.41$  pvalue=0.001, respectively) (see RDA analyses in **Fig. S9**). Specific chemical  
359 compounds were the main contributors to these correlations (*i.e.* the polyols, MSA and  $\text{Na}^+$   
360 for the fungal communities, and organic carbon,  $\text{Na}^+$ ,  $\text{Cl}^-$  and erythriol for the bacterial  
361 communities). Consistent with seasonal patterns observed for both microbial community  
362 structures and chemical composition, we observed strong positive and negative correlations  
363 between the concentration of some chemical compounds and the relative abundances of  
364 bacterial genera or fungal species. For examples, mannitol-arabitol and *Alternaria sp.*  
365 **BMP\_2012** ( $r=0.73$  and pvalue= $4.8 \times 10^{-9}$ ) and mannitol-arabitol and *Pseudotaeniolina*  
366 *globosa* ( $r=-0.66$  and pvalue= $5.6 \times 10^{-7}$ ) (**Table S7**).

367

### 368 *Weather characteristics: local meteorology and air mass geographical origin*

369 Temperature, wind speed and UV radiation (weekly averages) varied over the year  
370 (pvalue<0.05), conversely to wind direction and relative humidity. The mean weekly  
371 temperature varied between -5.5°C and 17.6°C (**Fig. S3**) and was significantly correlated to  
372 the season (pvalue= $1.4 \times 10^{-11}$  – **Fig. S10**). Wind speed varied between 2.8 and 13.5 m/s on  
373 average, and this was significantly higher in winter compared to summer and spring  
374 (pvalue= $2.1 \times 10^{-3}$ , **Fig. S10**), and significantly more variable in winter compared to the other  
375 seasons (pvalue= $5.4 \times 10^{-4}$ ). Wind speed and direction were positively correlated (r=0.44,  
376 pvalue=0.001) with stronger winds coming from West. Nevertheless, the mean wind direction  
377 was not significantly different between seasons (pvalue=0.11) and the air mass origins were  
378 only partially correlated to the seasons (16% and 14% of the variance explained,  
379 pvalue=0.013). The wind roses and the backtrajectory density plots for each season are  
380 presented in **Fig. S10** and **Fig. S11**. The seasonal weekly variability in wind conditions,  
381 temperature and relative humidity are shown in **Table S3**.

382 Bacterial concentration correlated best with UV radiation (r=0.38, pvalue= $5.4 \times 10^{-3}$ ) and  
383 fungal concentration correlated best with temperature (r=0.38, pvalue= $5.6 \times 10^{-3}$ ) (**Table S8**).  
384 A significant and strong correlation was also found between both the bacterial and fungal  
385 community structures and the overall meteorology (*i.e.* temperature, relative humidity, wind  
386 direction and speed) (r=0.57 pvalue=0.001 and r=0.48 pvalue=0.001). Bacterial richness was  
387 strongly correlated with temperature (r=0.52, pvalue= $7.7 \times 10^{-5}$ ) while fungal richness best  
388 correlated with wind direction (r=0.50, pvalue= $4.6 \times 10^{-4}$ ) (**Table S8**).

389

## 390 Discussion

391 *Seasonal variation in airborne microbial community composition due to changes in local*  
392 *landscapes*

393 Previous investigations of the temporal variations of airborne microbial communities have  
394 consistently shown a seasonal shift in both cell concentration and community structure<sup>2,9-12</sup>.  
395 This was explained mainly by changes in the surrounding landscape condition<sup>10,11,27</sup> (*e.g.*,  
396 vegetation in summer, snow cover in winter *etc.*), local meteorology<sup>2,9</sup> and/or the origin of the  
397 air masses (*i.e.* changes in the global air circulation)<sup>9</sup>. Our data showed that seasonality was  
398 correlated to the temporal distribution of airborne microbial community structure at puy de  
399 Dôme. With these results, we demonstrated the importance of local regional sources (*i.e.*  
400 within 50 km) even at relatively elevated sites such as puy de Dôme. Puy de Dôme is mainly  
401 surrounded by croplands and/or natural vegetation (> 80% of the surface within a 50 km  
402 perimeter based on MODIS satellite images; **Fig. 1**) that undergo strong changes over the year  
403 at such latitudes (see puy de Dôme monthly satellite images in **Fig. S1** for an overview).  
404 These changes are partly associated with crops (mainly wheat and grain maize) and vegetation  
405 that cycle through their different phases on an annual basis. Changes in landscape  
406 characteristics are themselves under direct influence of climatic conditions, including  
407 precipitation rate, temperature and sunlight exposure. This consequently has a critical  
408 influence on the surface microbial communities<sup>28,29</sup>. Over the year, different microorganisms  
409 with different trophic modes were likely aerosolized (**Fig. 3**). Fungal phytopathogens (like  
410 *Ustilago hordei*) and leaf-associated fungi (like *Naevula minutissima*) increased in relative  
411 abundance during the spring and summer periods when the crop plants grew and trees were  
412 green; while saprotrophs (like *Cladophialora protea*) increased in relative abundance during  
413 the autumn and winter periods after crop harvesting and when dead and decomposing  
414 biological material covered terrestrial surfaces. Similar to fungi, soil-associated bacterial taxa  
415 (like *Hymenobacter*) were observed in higher relative abundance in autumn and winter and  
416 bacterial phytopathogens and leaf-associated bacteria (like *Sphingomonas*) were observed in  
417 higher relative abundance in spring and summer. The three general trends (*i.e.* an increase of

418 specific taxa in autumn/winter; an increase of other taxa in summer/spring; stable or randomly  
419 variable microbial taxa over the year – **Fig. 4**) might have driven the distribution of the  
420 samples based on both the airborne bacterial and fungal community structures in two major  
421 clusters (*i.e.* an autumn/winter cluster versus a spring/summer cluster observed in **Fig. 2**). In  
422 addition, the period during which we observed an increase in the relative abundance of a  
423 winter or summer-associated microbial taxon varied in length and might have been specific to  
424 the life strategy of the given taxon. Microbial taxa whose relative abundance remained stable  
425 or varied randomly over the year might partly belong to taxa associated to decomposing  
426 matter (the trophic mode of all the fungal taxa present in this group was saprotroph) that is  
427 present the whole year. Airborne fungal community structure showed a stronger seasonal  
428 variation than bacterial community structure did, likely related to a higher number of fungal  
429 taxa showing a seasonal pattern as compared to bacterial taxa (40/50 and 31/50 for fungi and  
430 bacteria, respectively). The stronger seasonal shift observed in airborne fungi might be  
431 explained by a greater influence of vegetation on fungi as compared to bacteria<sup>30</sup>.

432

#### 433 *Role of local meteorology in the intraseasonal variability of airborne microbial community* 434 *composition*

435 Local meteorology might also play a role in the temporal distribution of airborne microbial  
436 communities at puy de Dôme especially on their intraseasonal variability. In a previous study  
437 considering numerous sampling sites<sup>1</sup>, we highlighted the importance of local meteorology  
438 (especially wind speed, wind direction and temperature variability over time) on the  
439 variability of airborne microbial communities when the site was surrounded by a variety of  
440 landscapes. Puy de Dôme is characterized by strong wind speeds and highly variable  
441 meteorological conditions partly explained by its central position and its high elevation within  
442 the Chaîne des Puys mountain range (+1465 m altitude above sea level and up to 500 m above

443 surrounding landscapes). The wind direction changed rapidly both within and between the  
444 weeks. The relative humidity and temperature also showed a high variability within and  
445 between the weeks within the same season (**Table S3**). While the correlation between  
446 meteorological parameters and airborne microbial communities at puy de Dôme is mainly  
447 explained by seasonality, local meteorological parameters might have also affected airborne  
448 microbial structures by influencing the aerosolization process as discussed in Tignat-Perrier et  
449 al. (2019)<sup>1</sup>. For example, specific temperatures might activate the sporulation of specific  
450 fungi<sup>31</sup>. The high correlation observed between temperature and airborne bacterial richness  
451 might be explained by the increased turbulence in air, a higher microbial diversity in the  
452 sources (*i.e.* surrounding landscapes)<sup>32–35</sup> as well as a drier surface favoring cell and biofilm  
453 detachment. Wind parameters were the meteorological parameters that best correlated to  
454 airborne fungal richness. Stronger winds are obviously more likely to aerosolize particles  
455 from surfaces.

456

457 *Minor contribution of distant sources in the temporal variation of airborne microbial*  
458 *communities*

459 Weekly averages of wind direction and origin of the air masses did not drastically change  
460 throughout the seasons and were highly and randomly variable over the year (**Fig. S10** and  
461 **S11**). We did not observe correlations between airborne microbial community structure and  
462 the origin of the air masses. In winter, during which free troposphere air masses, and thus  
463 potentially long-range transport, have a larger influence<sup>36–38</sup>, the variability in the bacterial  
464 community structure was not the highest. Marine air masses have been shown to prevail  
465 (72%) during winter at puy de Dôme<sup>38</sup>. One sample showed an especially strong marine  
466 signature in terms of chemistry (February 2<sup>nd</sup>, 2017). However, this sample has similar  
467 proportion of marine bacterial genera (*Corialomargarita*, *Rubritalea*, *Aquimarina*) as other



468 samples. Whenever present, the identified specific marine bacterial genera were very rare  
469 (they were represented by only 2 or 3 sequences over > 20000 sequences per sample). Unlike  
470 previous suggestions for cloud water-associated microorganisms at this site, microbial  
471 communities in the dry phase did not seem to mainly originate from oceanic sources<sup>27</sup>. Uetake  
472 et al. (2019)<sup>2</sup> investigated airborne (not cloud-associated) microbial communities in Tokyo  
473 (Japan) over a year and also highlighted the absence of oceanic related bacteria (*i.e.* SAR  
474 group, *Oceanospirillales*) that would have suggested transport of airborne microbial cells  
475 from the Pacific Ocean to Tokyo.

476 We also observed a seasonal change in the particulate matter chemistry (PM10 chemistry)  
477 (Fig. S7). At puy de Dôme, changes in PM10 chemistry throughout the seasons were  
478 correlated to changes in air mass origins (local and distant) and changes in the vertical  
479 stratification of the atmospheric layers (such as the increase of the height of the mixed layer in  
480 summer)<sup>36,37</sup>. We observed specific and strong correlations between some chemical species  
481 and microbial taxa (Table S7) and this could explain the overall correlation between the  
482 overall PM10 chemistry and airborne microbial structure. In particular, we observed  
483 correlations between specific microbial taxa and polyols. The concentration of atmospheric  
484 polyols might be due to the presence of airborne green plant debris as well as specific  
485 microbial taxa and especially fungal taxa which produce polyols<sup>39-42</sup>. Our sampling strategy  
486 (one-week sampling) might not have been adapted to identify microbial long-range transport  
487 events that, if they occurred, might have been greatly diluted by the local sources.  
488 Investigations on the temporal variability of airborne microbial communities that concluded  
489 the significant contribution of distant sources in the composition of airborne microbial  
490 communities<sup>9,13</sup> had either a different sampling strategy than ours (*i.e.* shorter sampling  
491 duration such as 24 h<sup>9</sup>) or did not sample microorganisms of the dry phase of the  
492 troposphere<sup>13</sup>.

493

494

#### 495 Conclusion

496 We investigated changes in airborne microbial community concentration and structure at the  
497 elevated continental site puy de Dôme in the Massif Central of France (+1465 m altitude  
498 above sea level) as a function of the local meteorology and particulate matter chemistry. We  
499 showed that puy de Dôme airborne microbial community structure likely shifted throughout  
500 the year in relation to the seasonal changes in surface conditions of the surrounding landscape  
501 of the mountain that was characterized mainly by croplands and natural vegetation. The  
502 microbial taxa that drove the seasonal distribution of airborne microbial communities showed  
503 different trends throughout the seasons depending on their trophic mode. Crop-associated  
504 microorganisms and especially crop pathogens were in higher relative abundance in  
505 spring/summer while soil-associated microorganisms and dead material-associated  
506 microorganisms were found in higher relative abundance in autumn/winter. Changes in the  
507 vertical stratification of the atmospheric layers throughout the seasons (such as the increase of  
508 the height of the mixed layer in summer) might also play a role in the seasonal shift of puy de  
509 Dôme airborne microbial communities. Within the different seasons, the temporal variability  
510 observed in the composition of airborne microbial communities was likely associated to the  
511 variable and windy meteorological conditions observed in puy de Dôme.

512

#### 513 Acknowledgements

514 This program was funded by ANR-15-CE01-0002–INHALE, Région Auvergne-Rhône Alpes  
515 and CAMPUS France. The chemical analyses were performed at the IGE AirOSol platform.  
516 We thank L.Pouilloux for computing assistance and maintenance of the Newton  
517 supercalculator.

518

519 Competing interests

520 The authors declare no competing interests.

521

522 Data availability

523 Sequences reported in this paper have been deposited in [ftp://ftp-adn.ec-](ftp://ftp-adn.ec-lyon.fr/aerobiology_Puy-de-Dome_amplicon_INHALE/)  
524 [lyon.fr/aerobiology\\_Puy-de-Dome\\_amplicon\\_INHALE/](ftp://ftp-adn.ec-lyon.fr/aerobiology_Puy-de-Dome_amplicon_INHALE/). A file has been attached explaining  
525 the correspondence between file names and samples.

526

527 Author contribution

528 AD, PA, CL and TMV designed the experiment. PA, AT, MJ and KS conducted the sampling  
529 field campaign. RTP did the molecular biology, bioinformatics and statistical analyses. RTP,  
530 AD, CL, TMV analyzed the results. RTP, TM, AD, PA and CL wrote the manuscript. All  
531 authors reviewed the manuscript.

532

533 References

- 534 1. Tignat-Perrier, R. *et al.* Global airborne microbial communities controlled by surrounding  
535 landscapes and wind conditions. *Sci Rep* **9**, 1–11 (2019).
- 536 2. Uetake, J. *et al.* Seasonal changes of airborne bacterial communities over Tokyo and influence of  
537 local meteorology. *bioRxiv* 542001 (2019) doi:10.1101/542001.
- 538 3. Amato, P. *et al.* A fate for organic acids, formaldehyde and methanol in cloud water: their  
539 biotransformation by micro-organisms. *Atmospheric Chemistry and Physics* **7**, 4159–4169 (2007).
- 540 4. Väitilingom, M. *et al.* Contribution of Microbial Activity to Carbon Chemistry in Clouds. *Appl*  
541 *Environ Microbiol* **76**, 23–29 (2010).
- 542 5. Ariya, P. A., Nepotchatykh, O., Ignatova, O. & Amyot, M. Microbiological degradation of  
543 atmospheric organic compounds. *Geophysical Research Letters* **29**, 34-1-34-4 (2002).

- 544 6. Pöschl, U. *et al.* Rainforest Aerosols as Biogenic Nuclei of Clouds and Precipitation in the  
545 Amazon. *Science* **329**, 1513–1516 (2010).
- 546 7. Brown, J. K. M. & Hovmøller, M. S. Aerial dispersal of pathogens on the global and continental  
547 scales and its impact on plant disease. *Science* **297**, 537–541 (2002).
- 548 8. Mhuireach, G. Á., Betancourt-Román, C. M., Green, J. L. & Johnson, B. R. Spatiotemporal  
549 Controls on the Urban Aerobiome. *Front. Ecol. Evol.* **7**, (2019).
- 550 9. Innocente, E. *et al.* Influence of seasonality, air mass origin and particulate matter chemical  
551 composition on airborne bacterial community structure in the Po Valley, Italy. *Sci. Total Environ.*  
552 **593–594**, 677–687 (2017).
- 553 10. Bowers, R. M., McCubbin, I. B., Hallar, A. G. & Fierer, N. Seasonal variability in airborne  
554 bacterial communities at a high-elevation site. *Atmospheric Environment* **50**, 41–49 (2012).
- 555 11. Bowers, R. M. *et al.* Seasonal variability in bacterial and fungal diversity of the near-surface  
556 atmosphere. *Environ. Sci. Technol.* **47**, 12097–12106 (2013).
- 557 12. Franzetti, A., Gandolfi, I., Gaspari, E., Ambrosini, R. & Bestetti, G. Seasonal variability of  
558 bacteria in fine and coarse urban air particulate matter. *Appl. Microbiol. Biotechnol.* **90**, 745–753  
559 (2011).
- 560 13. Cáliz, J., Triadó-Margarit, X., Camarero, L. & Casamayor, E. O. A long-term survey unveils  
561 strong seasonal patterns in the airborne microbiome coupled to general and regional atmospheric  
562 circulations. *Proc. Natl. Acad. Sci. U.S.A.* **115**, 12229–12234 (2018).
- 563 14. Amato, P. *et al.* Metatranscriptomic exploration of microbial functioning in clouds. *Sci Rep* **9**, 1–  
564 12 (2019).
- 565 15. Amato, P. *et al.* Active microorganisms thrive among extremely diverse communities in cloud  
566 water. *PLOS ONE* **12**, e0182869 (2017).
- 567 16. Amato, P. *et al.* Survival and ice nucleation activity of bacteria as aerosols in a cloud simulation  
568 chamber. *Atmospheric Chemistry and Physics* **15**, 6455–6465 (2015).
- 569 17. Väitilingom, M. *et al.* Potential impact of microbial activity on the oxidant capacity and organic  
570 carbon budget in clouds. *PNAS* **110**, 559–564 (2013).

- 571 18. Dommergue, A. *et al.* Methods to investigate the global atmospheric microbiome. *Front.*  
572 *Microbiol.* **10**, (2019).
- 573 19. Masella, A. P., Bartram, A. K., Truszkowski, J. M., Brown, D. G. & Neufeld, J. D. PANDAseq:  
574 paired-end assembler for illumina sequences. *BMC Bioinformatics* **13**, 31 (2012).
- 575 20. Wang, Q., Garrity, G. M., Tiedje, J. M. & Cole, J. R. Naive Bayesian Classifier for Rapid  
576 Assignment of rRNA Sequences into the New Bacterial Taxonomy. *Applied and Environmental*  
577 *Microbiology* **73**, 5261–5267 (2007).
- 578 21. Deshpande, V. *et al.* Fungal identification using a Bayesian classifier and the Warcup training set  
579 of internal transcribed spacer sequences. *Mycologia* **108**, 1–5 (2016).
- 580 22. Nguyen, N. H. *et al.* FUNGuild: An open annotation tool for parsing fungal community datasets  
581 by ecological guild. *Fungal Ecology* **20**, 241–248 (2016).
- 582 23. Draxler, R. R. & Hess, G. D. An Overview of the HYSPLIT\_4 Modelling System for Trajectories,  
583 Dispersion, and Deposition. 25.
- 584 24. Carslaw, D. Tools for the Analysis of Air Pollution Data. (2019).
- 585 25. Dray, S., Dufour, A.-B. & Thioulouse, J. Analysis of Ecological Data: Exploratory and Euclidean  
586 Methods in Environmental Science. (2018).
- 587 26. Harrell, F. E. & Dupont, C. Harrell Miscellaneous - Package ‘Hmisc’. (2019).
- 588 27. Amato, P. *et al.* An important oceanic source of micro-organisms for cloud water at the Puy de  
589 Dôme (France). *Atmospheric Environment* **41**, 8253–8263 (2007).
- 590 28. Zhang, Q. *et al.* Alterations in soil microbial community composition and biomass following  
591 agricultural land use change. *Scientific Reports* **6**, 36587 (2016).
- 592 29. Constancias, F. *et al.* Mapping and determinism of soil microbial community distribution across  
593 an agricultural landscape. *Microbiologyopen* **4**, 505–517 (2015).
- 594 30. Sun, S., Li, S., Avera, B. N., Strahm, B. D. & Badgley, B. D. Soil Bacterial and Fungal  
595 Communities Show Distinct Recovery Patterns during Forest Ecosystem Restoration. *Appl*  
596 *Environ Microbiol* **83**, (2017).
- 597 31. Pickersgill, D. A. *et al.* Lifestyle dependent occurrence of airborne fungi. *Biogeosciences*  
598 *Discussions* 1–20 (2017) doi:<https://doi.org/10.5194/bg-2017-452>.

- 599 32. Dennis, P. G., Newsham, K. K., Rushton, S. P., O'Donnell, A. G. & Hopkins, D. W. Soil bacterial  
600 diversity is positively associated with air temperature in the maritime Antarctic. *Sci Rep* **9**, 1–11  
601 (2019).
- 602 33. Zhou, J. *et al.* Temperature mediates continental-scale diversity of microbes in forest soils. *Nature*  
603 *Communications* **7**, 12083 (2016).
- 604 34. Nottingham, A. T. *et al.* Microbes follow Humboldt: temperature drives plant and soil microbial  
605 diversity patterns from the Amazon to the Andes. *Ecology* **99**, 2455–2466 (2018).
- 606 35. Tittensor, D. P. *et al.* Global patterns and predictors of marine biodiversity across taxa. *Nature*  
607 **466**, 1098–1101 (2010).
- 608 36. Venzac, H., Sellegri, K., Villani, P., Picard, D. & Laj, P. Seasonal variation of aerosol size  
609 distributions in the free troposphere and residual layer at the puy de Dôme station, France.  
610 *Atmospheric Chemistry and Physics* **9**, 1465–1478 (2009).
- 611 37. Bourcier, L., Sellegri, K., Chausse, P., M. Pichon, J. & Laj, P. Seasonal variation of water-soluble  
612 inorganic components in aerosol size-segregated at the puy de Dôme station (1,465 m a.s.l.),  
613 France. *Journal of Atmospheric Chemistry* **69**, (2012).
- 614 38. Freney, E. J. *et al.* Seasonal variations in aerosol particle composition at the puy-de-Dôme  
615 research station in France. *Atmospheric Chemistry and Physics* **11**, 13047–13059 (2011).
- 616 39. Medeiros, P. M., Conte, M. H., Weber, J. C. & Simoneit, B. R. T. Sugars as source indicators of  
617 biogenic organic carbon in aerosols collected above the Howland Experimental Forest, Maine.  
618 *Atmospheric Environment* **40**, 1694–1705 (2006).
- 619 40. Ruijter, G. J. G. *et al.* Mannitol Is Required for Stress Tolerance in *Aspergillus niger*  
620 *Conidiospores*. *Eukaryot Cell* **2**, 690–698 (2003).
- 621 41. Solomon, P. S., Waters, O. D. C. & Oliver, R. P. Decoding the mannitol enigma in filamentous  
622 fungi. *Trends Microbiol.* **15**, 257–262 (2007).
- 623 42. Lewis, D. H. & Smith, D. C. Sugar alcohols (polyols) in fungi and green plants. *New Phytologist*  
624 **66**, 143–184 (1967).
- 625

